



## Projected Curve Number (CN) Changes and Surface Runoff Response to Corrected Land Cover Dynamics in the Citarum-Majalaya Catchment

Dadang Ruhiat<sup>1\*</sup>, Indratmo Soekarno<sup>2</sup>, Hadi Kardhana<sup>2</sup>, Rusmawan Suwarman<sup>3</sup>

<sup>1</sup> Civil Engineering Doctoral Program, Bandung Institute of Technology, Bandung 40132, Indonesia

<sup>2</sup> Department of Civil Engineering, Faculty of Civil and Environmental Engineering, Bandung Institute of Technology, Bandung 40132, Indonesia

<sup>3</sup> Faculty of Earth Sciences and Technology, Bandung Institute of Technology, Bandung 40132, Indonesia

Corresponding Author Email: [dadangwiraruhiat@gmail.com](mailto:dadangwiraruhiat@gmail.com)

Copyright: ©2025 The authors. This article is published by IETA and is licensed under the CC BY 4.0 license (<http://creativecommons.org/licenses/by/4.0/>).

<https://doi.org/10.18280/ij dne.200407>

### ABSTRACT

**Received:** 22 March 2025

**Revised:** 20 April 2025

**Accepted:** 25 April 2025

**Available online:** 30 April 2025

#### Keywords:

*curve number, surface runoff, land cover, trend model, SCS-CN method*

Land use and land cover changes that occur rapidly and without proper control have the potential to increase runoff discharge and elevate the risk of flooding. This study is crucial for analyzing land cover changes that influence runoff discharge, evaluating potential future scenarios, and providing a scientific foundation for the formulation of policy recommendations. The assessment of land cover changes on surface runoff is carried out by observing variations in Curve Number (CN) values. The analysis and projection of CN values are based on corrected land cover map data and trend models. Two projection approaches are used: the first assumes no mitigation efforts, while the second is based on spatial planning strategies. The first approach yields a higher CN value and shows an increasing trend, with an estimated CN value of 81.52 in 2044, rising to 82.17 by 2050. The second approach yields a Curve Number (CN) value of 79.87 in 2044, which increases slightly to 79.93 by 2050 (still below 80.00). The difference in maximum runoff between the two approaches continues to grow, from 0.11 m<sup>3</sup>/s in 2025 to 0.51 m<sup>3</sup>/s in 2044. Land cover changes based on spatial planning scenarios demonstrate a significant reduction in CN values and surface runoff.

## 1. INTRODUCTION

Changes in land cover are inevitable along with population growth and demands for land. This condition places additional hydrological stress on watershed systems. This phenomenon is evident in the increasing frequency of flooding observed in the downstream areas of the Citarum-Majalaya catchment, including the Majalaya urban area [1], Bandung City, Bandung Regency, and West Bandung Regency [2]. These observations represent empirical evidence that cannot be denied.

Land use/cover is a dynamic component of watershed characteristics that directly reflects the magnitude of the influence of human activities [3]. Land use refers to how humans utilize and manage land and its resources to sustain their livelihoods [4]. While land cover refers to the biological and physical materials that exist on the land surface, both natural and manmade [5]. Land cover changes encompass both natural and man-made alterations that occur over time. Land use and land cover are considered to be the result of the natural and socio-economic aspects of an area and the accompanying anthropogenic manipulations in space and time [6]. Previous research [2, 7, 8], conducted in the upstream Citarum watershed, concluded that uncontrolled land use/cover will increase runoff discharge and significantly increase the risk of flood hazards as indicated by an increase in maximum river

discharge. Increased frequency of flooding in Bandung City, Bandung Regency, and West Bandung Regency [2] as the downstream area of the Upper Citarum watershed is thought to be related to the intensity of land cover changes. Apart from the impact on flood frequency, other research [9] also concluded that changes in land cover contributed significantly to reducing low flow in the upper Citarum watershed. In other words, changes in residential land cover, which are rapidly increasing, and forest land, which tends to decrease in the long term, will have an impact on water availability in the Bandung basin area. However, this study focuses on examining how, and to what extent, the intensity of land cover change affects surface runoff, as well as projecting its future impact.

Assessing the impact of land cover changes on surface runoff can be done through the approach of observing changes in Curve Number (CN) values. CN is an important factor in the Soil Conservation Service-Curve Number (SCS-CN) method, where in this method, the characteristics of the water catchment area are the basic parameters for determining surface runoff [10]. This method is a popular empirical method for estimating surface runoff from rainfall events at the watershed scale. CN is an integration of the influence of soil type, land cover, land management, hydrological conditions, and soil moisture conditions [11-13]. Determining the CN value has more accuracy if the process uses an accurate land cover map. The step of correcting the land cover map is

important to eliminate errors, until a land cover map is obtained according to actual conditions. The correction process can use the Geographic Information System (GIS) method, which is designed to facilitate the processing of spatial data and non-spatial data [10].

Numerous studies conducted in various regions have demonstrated that land cover changes, such as the conversion of forests to agricultural land, agricultural land to settlements, and both forests and agricultural areas to urban land, lead to an increase in built-up areas and a corresponding decrease in forest cover. These transformations significantly influence hydrological responses, resulting in increased Curve Number (CN) values, surface runoff, and peak flood discharge [14–17]. In the National Capital Region (IKN), forest-to-urban land conversion is projected to increase CN values by 10–15% over a 15-year period (2020–2035), contributing to a 10% rise in both peak discharge and runoff volume by 2035 [18]. Moreover, the conversion of every 13 km<sup>2</sup> of forest and agricultural land to urban areas is estimated to elevate peak flood discharge by 4.63% and runoff volume by 4.34% [19]. Supporting these findings, research in other locations also indicates that land cover changes affect CN values and baseflow discharge [20].

This research will explain more accurately the related assumption that controlled and spatially appropriate land use/land cover will significantly reduce the CN value and reduce the risk of losses due to increased surface runoff. Although studies regarding changes in land cover, CN values, rainfall and surface runoff at this study location have been carried out in previous research [2], this research uses land cover map data that has not been corrected so it is feared that significant errors will occur between the analysis results and the actual conditions of land cover and CN values. The novelty of this research is the analysis and projection of CN values at the study location using corrected land cover and land cover scenarios based on spatial planning, and calculating surface

runoff predictions using rainfall data forecast using the ANN method. Research in the form of assessments and forecasts related to the impact of changes in land use/land cover has been carried out in another study [21], but this study focuses more on discussing other environmental parameters, namely variations in carbon availability in response to changes in land use/land cover.

The main objective of this research is to analyze land cover changes, make projections of CN values in the Citarum-Majalaya catchment from 2024-2050, and analyze the impact on surface runoff. Two projection approaches are employed. The first assumes that no mitigation efforts will be implemented regarding land cover change. The second follows a scenario based on spatial planning compliance.

This research holds significant practical value, particularly in the fields of land use planning and flood risk management. In the context of land use planning, this study provides quantitative information on the relationship between land cover changes and Curve Number (CN) values, which directly influence surface runoff volume. This information can serve as a foundation for land use planning decisions, such as preventing the conversion of green spaces into built-up areas in regions with high CN values, identifying priority conservation zones, and developing simulations of future land use change scenarios. In terms of flood risk management, the findings of this study enable more accurate surface runoff estimations by using CN values adjusted for land cover dynamics. Consequently, flood-prone areas can be identified more precisely by combining land cover change data with the increased potential for runoff.

## 2. MATERIALS AND METHODS

### 2.1 Study area

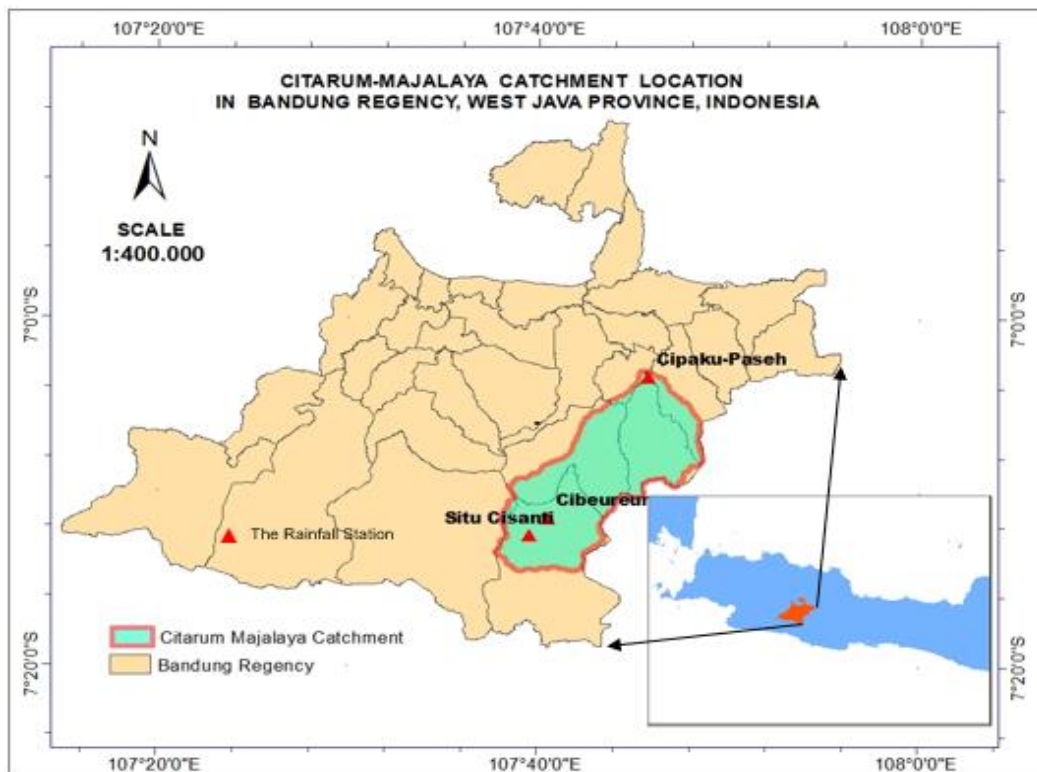


**Figure 1.** The study area and the rainfall station distribution

The study location is a catchment area of the Citarum-Majalaya stream gauging station (around 204.52 km<sup>2</sup>) and is part of the upstream Citarum sub-watershed (around 269.43 km<sup>2</sup>). The catchment is geographically located between 7°3'1.96"-7°14'33.1"S and 107°37'50.7"-107°48'40.8"E, and administratively is part of the Bandung District, West Java Province, Indonesia. The distribution of the catchment area is in 6 subdistricts, namely the majority are in Kertasari Subdistrict (33.5%), Pacet Subdistrict (30.8%), Ibun Subdistrict (26.6%), and a small portion is in Majalaya Subdistrict, Pangalengan Subdistrict, and Paseh Subdistrict. The location of the catchment in Bandung District can be seen in Figure 1.

## 2.2 Land cover

The land cover map of the study location was created and corrected using the ArcGIS 10.7.1 software application for 2000 to 2021. The basic data in shapefile format from 2000-2021 was obtained from the Ministry of Environment and Forestry of the Republic of Indonesia. Land cover map data is

corrected before being used further for land cover change analysis. Corrections are carried out for validation and to avoid errors in interpretation, so that land cover data is obtained with good accuracy. The land cover maps of the study area before correction, for the years 2000 and 2021, are presented in Figure 2.

Land use/cover and conservation structures (water and soil) greatly influence surface runoff [22], and in this research will be more on discussing the effect of land cover changes on runoff. Analysis of land cover changes in this location was carried out for 22 years (2000-2021). The land cover of this location was classified based on SNI 7645-2010 concerning land cover classification [23], namely forest, shrubs, plantation, settlements (built environment), open land, water bodies, dryland farming, and ricefields. Land cover influences identifying flood-prone zones and directly impacts infiltration rates [24]. Impervious surfaces in the settlement (built environment) can increase runoff and reduce water infiltration [25]. This analysis is conducted to obtain information on the pattern of change for each type of land cover, which becomes the basis for projecting changes and estimating CN values.

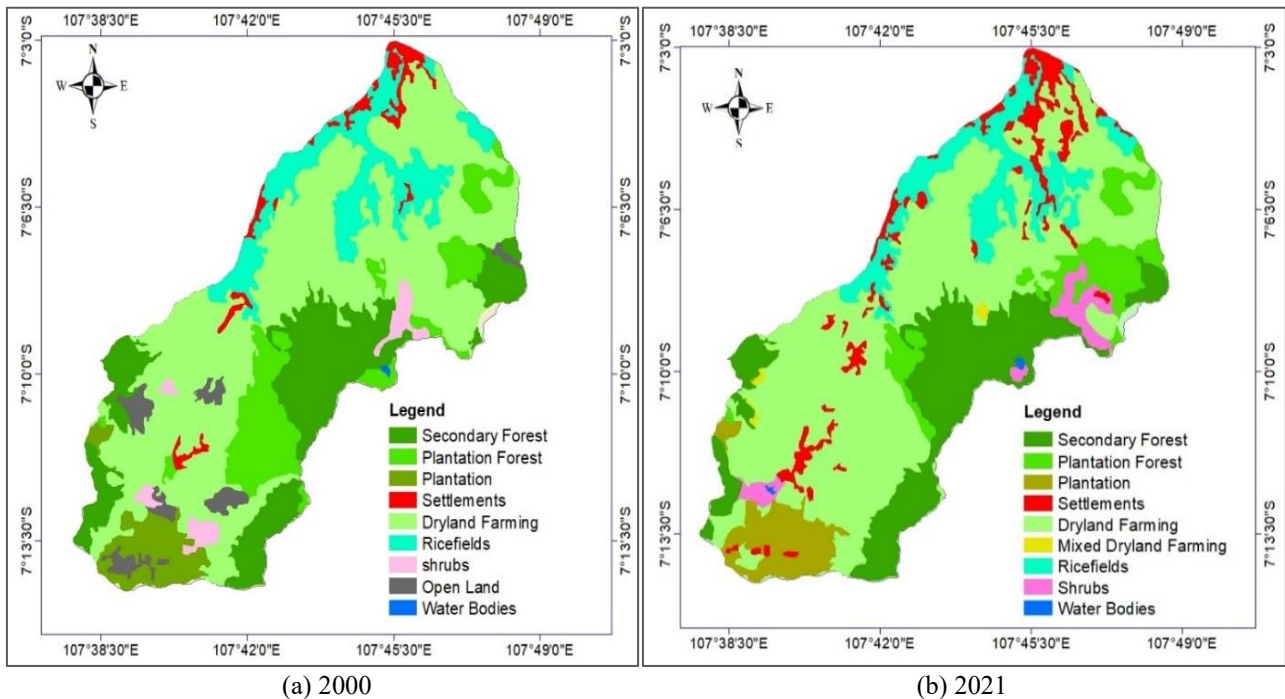


**Figure 2.** The land cover maps of the study area before correction

This study will also analyze the variation in land cover between 2000-2021, which is divided into several phases, namely 2000, 2006, 2012, 2018, and 2021. Variations in land cover changes are quantified using the dynamic degree of single land cover  $k$  and the dynamic degree of comprehensive land use  $L_c$ . The  $K$  reflects the level of annual variation in the area of a type of land between the initial and final phases, and  $L_c$  reflects the comprehensive annual variation level of the area of all land types. The positive  $K$  and  $L_c$  value indicate that the area of land cover type increases, and if the value is negative, then the area of land cover type decreases. The greater the absolute value of  $K$  and  $L_c$ , the more significant the variation. The  $K$  and  $L_c$  value can be calculated using the Turner method [4, 26], with the formula as in Eqs. (1) and (2).

$$K = \frac{U_b - U_a}{U_a} \times \frac{1}{T} \times 100\% \quad (1)$$

$$L_c = \frac{\sum_{i=1}^n |U_{bi} - U_{ai}|}{2 \sum_{i=1}^n U_{ai}} \times \frac{1}{T} \times 100\% \quad (2)$$

where,  $U_a$  and  $U_b$  are the area of land type in the initial and final phases;  $T$  is the length of the sample period (unit: year);  $n$  is the number of land types in the study area.

## 2.3 Rainfall

Rainfall analysis in this study utilizes precipitation data collected from three rainfall stations located around the study area, namely the Cibereum Station (area of influence: 87.8 km<sup>2</sup>), the Cipaku-Paseh Station (area of influence: 84.4 km<sup>2</sup>), and the Situ Cisanti Station (area of influence: 31.6 km<sup>2</sup>). The spatial distribution of these stations, the availability of data, and their respective areas of influence are illustrated in Figure

1 and summarized in Table 1. The rainfall data were obtained from the Hydrology and Water Environment Center, Directorate General of Water Resources, Ministry of Public Works and Housing, Republic of Indonesia. Due to the spatial and temporal variability of rainfall, it is necessary to express

the data in the form of regional rainfall, which in this study is calculated using the Thiessen polygon method (Figure 3). For analytical purposes, the regional daily rainfall data were subsequently converted into monthly values, with the average rainfall for the period 2000–2021 presented in Figure 4.

**Table 1.** Rainfall data availability

Rainfall Station	Longitude	Latitude	Data Availability	Influence Area
Cibeureum	107.677	-7.192	2002-2021	41.40%
Cipaku-Paseh	107.764	-7.057	2002-2021	43.10%
Situ Cisanti	107.661	-7.208	2014-2021	15.50%

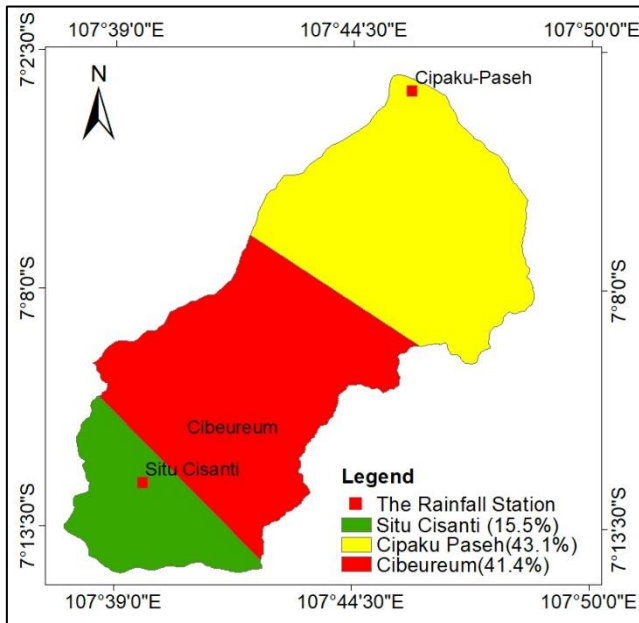


**Figure 3.** The rainfall station and the Thiessen Polygon

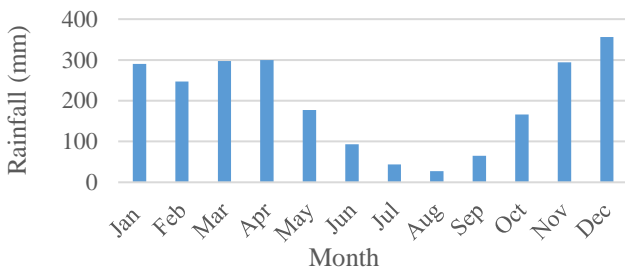


**Figure 4.** The monthly average regional rainfall

**2.4 Hydrologic soil group**

The Hydrologic Soil Group (HSG) map of the study area is derived from the broader HSG map of the Citarum Watershed. The map data, provided in shapefile format, were obtained from the Oak Ridge National Laboratory Distributed Active Archive Center (ORNL DAAC), NASA [27]. The HSG map specific to the study area (Figure 5) was generated through a Geographic Information System (GIS) process, involving an intersection between the study area boundary (Citarum-Majalaya catchment) and the HSG map of the Citarum Watershed. Subsequently, an overlay analysis was performed between the HSG map and the land cover map of the study area to generate Hydrologic Response Unit (HRU) data. These HRU data serve as the basis for calculating the composite

Curve Number (CN) values within the study area.

HSG classification based on soil texture class, along with runoff potential, is presented in Table 2 [27]. The four standard classes, namely A, B, C, and D, correspond to soils with low, moderately low, moderately high, and high runoff potential, respectively. Wet soils have high runoff potential (regardless of texture) due to the presence of a groundwater table within 60 cm of the surface [27]. Wet soils have a dual HSG (e.g., HSG A/D): they can act as HSG A or HSG D depending on drainage conditions or groundwater levels. This usually occurs when the surface soil has high infiltration characteristics (HSG A), but the subsoil has very low permeability (HSG D), which can cause water to pool or drain slowly.

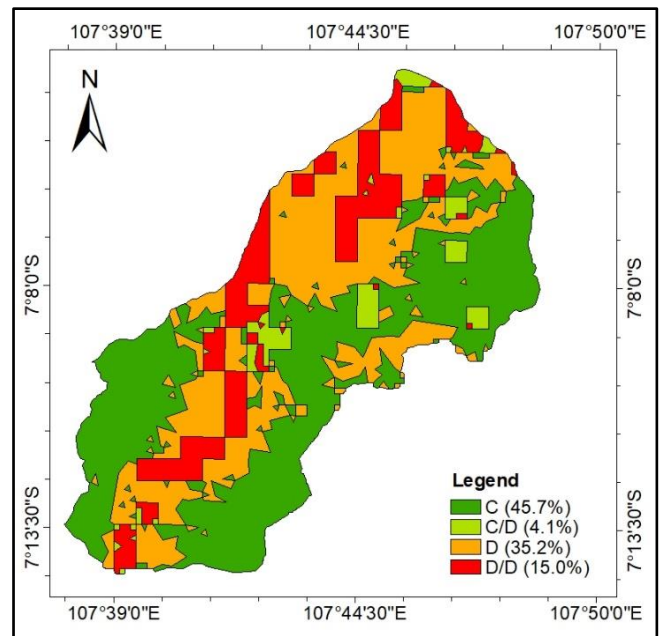


**Figure 5.** The HSG map of the study location

**Table 2.** HSG classification based on soil texture class

HSG	Soil Texture Class	Runoff Potential
A	Sand	Low
B	Sandy loam, loamy sand	Moderately low
C	Clay loam, silty clay loam, sandy clay loam, loam, silty loam, silt	Moderately high
D	Clay, silty clay, sandy clay	High
A/D	Sand	High
B/D	Sandy loam, loamy sand	High
C/D	Clay loam, silty clay loam, sandy clay loam, loam, silty loam, silt	High
D/D	Clay, silty clay, sandy clay	High

Source: Study [27].

## 2.5 Methods

This research calculates the CN value and its projections using two approaches. The first is the assumption that there is no effort (do nothing) related to land cover control and planning, and the second is the land cover change scenario based on the spatial pattern plan. The projected CN value for the first approach (do nothing) uses a trend model from the observed CN value and uses a scenario land cover change trend model to calculate the scenario CN.

The novelty of this research is the analysis and projection of

CN values at the study location using corrected land cover and land cover scenarios, as well as calculating surface runoff predictions using forecast rainfall data using the ANN method. The output of this research is surface runoff information based on scenario CN values and CN do nothing values. The output from these two approaches is then compared and analyzed. The results of this research can be used as recommendations for regional officials in formulating policies related to the preparation of spatial plans and natural resource management in their region. The research stage diagram is presented in Figure 6.

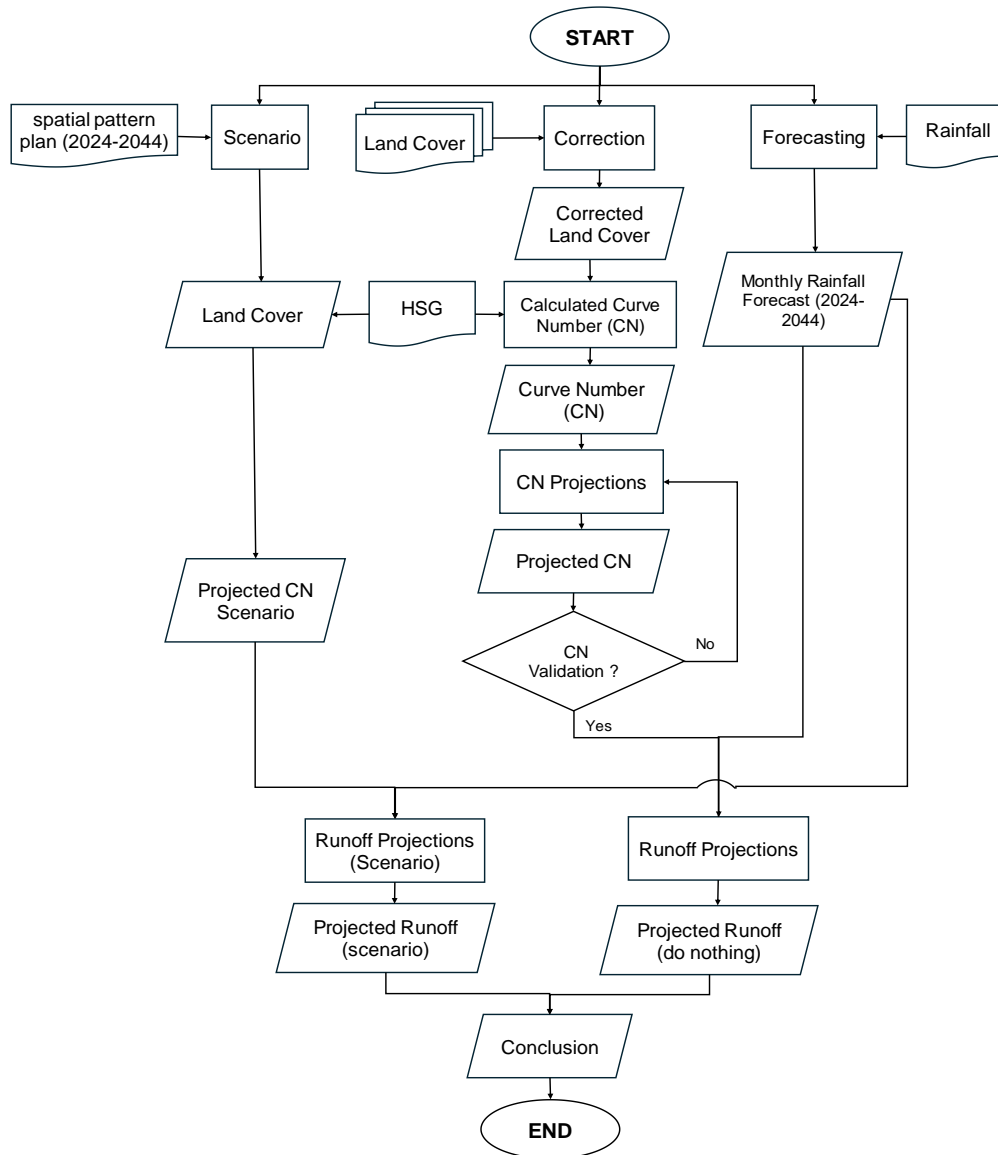


Figure 6. Flow chart of research stages

### 2.5.1 Analysis of changes in curve number

Curve number (CN) value describes the soil's ability to infiltrate and turn excess rain into surface runoff. The CN value of a watershed or catchment depends on the soil type and land cover. For catchments that consist of several soil types and land covers, composite CN can be used to estimate direct runoff using the following calculation method [28, 29].

$$CN = \frac{\sum A_i CN_i}{\sum A_i} \quad (3)$$

where, CN is the composite CN value,  $A_i$  is the subcatchment area  $i$ , and  $CN_i$  is the CN value of catchment area  $i$ . CN values range from 1 (minimum) to 100 (maximum) depending on the hydrological soil group HSG), land use/cover type, and previous soil moisture conditions [30]. Changes in the CN value of the study location were analysed from 2000 to 2021. Examples of overlay maps of land cover in 2021 and HSG are presented in Figure 7. The CN values for several HRU conditions are presented in Table 3 [31-33].

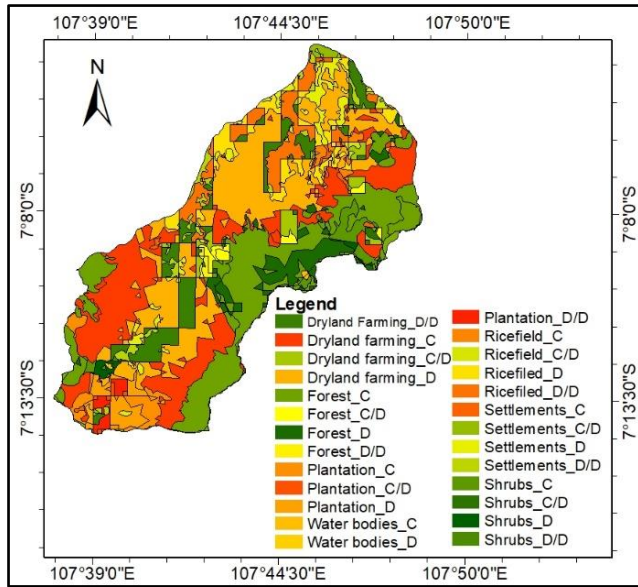


Figure 7. The HRU maps

Table 3. CN value for the hydrologic response unit

Type of Land Cover	HSG			
	A	B	C	D
Forest:				
- Poor forest cover (Rare plants)	45	66	77	83
- Forest cover is good	25	55	70	77
Plantation:				
- Bad condition	57	73	82	86
- Fair condition	43	65	76	82
- Good condition	32	58	72	79
Settlement	89	92	94	95
Drayland farming	64	75	83	85
Ricefield:				
- Bad condition	65	76	84	88
- Fair condition	64	75	83	87
- Good condition	63	75	83	87
Shrubs:				
- Bad condition	48	67	77	83
- Fair condition	35	56	70	79
- Good condition	30	48	65	77
Open land:				
- Good condition (grass covers 75% of the area)	39	61	74	80
- Fair condition (grass covers 50-75% of the area)	49	69	79	84
- water bodies	98	98	98	98

### 2.5.2 Projection of CN values

The analysis of changes in CN values in this research uses the trend method. This method is an analysis technique used to identify data patterns within a certain period and can be used to make predictions for the future. The model generally consists of a linear trend and a nonlinear trend. One of the advantages of the non-linear trend method is that it is excellent for predicting long-term data, and the forecast results are close to actual values [34]. The trend pattern of the CN value data series was detected over 22 years (2000-2021). The trend model for CN values can be expressed in a general equation as in Eq. (4), where  $t$  is time (year) and  $a_i$  are model coefficients [35]. If  $n=1$ , then the trend has a linear pattern; if  $n=2$  and  $n=3$ , then it has a quadratic and cubic polynomial pattern, respectively.

$$CN = \sum_{i=0}^n a_i t^i \quad (4)$$

$$R = \frac{n \sum xy - \sum x \sum y}{\sqrt{(n \sum x^2 - (\sum x)^2)(n \sum y^2 - (\sum y)^2)}} \quad (5)$$

The first step in trend analysis is to visualize data by making graphs or plots of data. This is done to detect data patterns over time as a basis for selecting an appropriate trend model. The best (most appropriate) trend model is determined based on the R-squared ( $R^2$ ) statistical criteria value. The best model is the one with  $R^2$  closest to 1. Then, based on the selected trend model, the CN value for the future is projected. The R calculation method is presented in Eq. (5). The R value measures the strength of the relationship between the projected CN and the actual CN, and  $R^2$  measures how well the model fits the actual CN data.

Table 4. Land cover of Bandung Regency according to the spatial pattern plan in 2044

No.	Penggunaan Lahan (kawasan)	km <sup>2</sup>	%
1	Water bodies	8.22	0.47
2	Settlements (Built environment)	391.53	22.46
3	Nature preserve	119.72	6.87
4	Horticulture	135.01	7.75
5	Protected forest	341.78	19.61
6	Production forest	4.07	0.23
7	Tourism	6.31	0.36
8	Plantation	394.90	22.66
9	Local protection	12.43	0.71
10	Defense and security	6.77	0.39
11	Industry	46.21	2.65
12	Stone mining	4.55	0.26
13	Fisheries & livestock cultivation	2.96	0.17
14	Buru Park	10.60	0.61
15	Crops	226.12	12.97
17	Great forest park & Nature tourism	31.84	1.83
	<b>Total</b>	<b>1743.04</b>	<b>100.00</b>

The projection of CN values in this research is based on two approaches. The first approach is the assumption that there will be no efforts regarding land cover change, and the second is a scenario based on spatial planning. The second approach is created based on spatial pattern plans by the Regional Regulation of Bandung Regency No. 1 of 2024 concerning Regional Spatial Planning of Bandung Regency 2024-2044. Maps and data of land cover plans are presented in Figure 8 and Table 4. Projections of CN values using the second approach were carried out to understand the impact of land cover changes on surface runoff.

Evaluation of model performance is carried out to determine the model's reliability by taking into account errors from predicted data to actual data. Model performance is measured using the statistical value criteria. These values are Mean Absolute Percentage Error (MAPE), Nash-Sutcliffe Efficiency (NSE), and Root Mean Square Error (RMSE). The MAPE value can be calculated using Eq. (6).

$$MAPE = \sum_{i=1}^n \left| \frac{y_i - \hat{y}_i}{y_i} \right| \times 100\% \quad (6)$$

RMSE measures the standard deviation of a model's prediction error; a smaller value means the model performs

better [36]. The RMSE value is calculated using Eq. (7). NSE is used as an index of suitability between calculated and observed data. The model fits very well if the NSE value is equal to 1, and it is poor if it approaches  $-\infty$  [37]. The NSE value is calculated using Eq. (8).

$$RMSE = \sqrt{\frac{1}{n} \sum_{i=1}^n \left( \frac{y_i - \hat{y}_i}{Y_i} \right)^2} \quad (7)$$

$$NSE = 1 - \frac{\sum_{i=1}^n (Y_i - \hat{y}_i)^2}{\sum_{i=1}^n (Y_i - \bar{y})^2} \quad (8)$$

where,  $Y_i$  = observation value;  $\hat{y}_i$  = model value.

The statistical test used in validating the CN value of the projection results is the student's t distribution test (t-test) to test the suitability of the model [26, 38], and using the MAPE statistical value criteria (4) in testing the model performance. Some of the t-test formulas used are shown in Eqs. (9) and (10).

A t-test is also employed to evaluate the differences in projected Curve Number (CN) values obtained from two distinct approaches.

$$t = \frac{|\bar{X}_1 - \bar{X}_2|}{\sigma \sqrt{\frac{1}{N_1} + \frac{1}{N_2}}} \quad (9)$$

$$\sigma = \sqrt{\frac{N_1 S_1^2 + N_2 S_2^2}{N_1 + N_2 - 2}} \quad (10)$$

where,  $t$ : the student's distribution (t-test);  $\bar{X}_i$ : mean CN of the  $i$ -th sample;  $\sigma$ : standard deviation of the population;  $N_i$ : size of the  $i$ -th sample, and  $S_i^2$ : variance of the  $i$ -th sample. The test hypothesis is two-way ( $H_1$ : Actual CN  $\neq$  Projected CN) with the following rejection criteria: Reject  $H_0$  if " $t_{count} < -t_{\alpha/2}(table)$ " or " $t_{count} > t_{\alpha/2}(table)$ ".

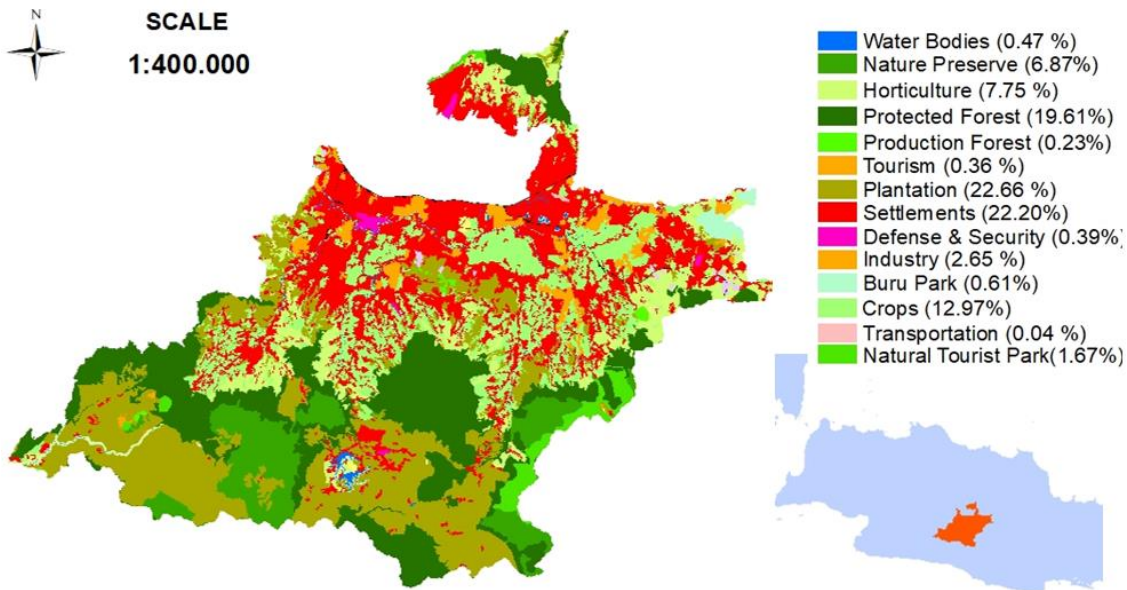


**Figure 8.** Spatial pattern plan of Bandung Regency based on the spatial plan 2024-2044

### 2.5.3 Forecasting monthly rainfall

Rainfall forecasting is carried out to predict monthly rainfall data in the Citarum-Majalaya catchment for 23 years (2022-2044). Then this rainfall data will be used to predict surface runoff discharge during that period. The rainfall forecasting process uses the Artificial Neural Network Backpropagation algorithm (ANN-BP). It is an information processing system with certain performance characteristics in common with biological neural networks [39]. It has advantages in terms of a small error rate and quite good generalization capabilities by using a training process according to weights to forecast future events [40]. This method was first introduced by Rumelhart et al. [41]. Backpropagation works by adjusting the weight values backwards based on the error value in the learning process [42]. The outline of the stages of ANN analysis with the backpropagation algorithm is: (1) analyze the number of hidden layer neurons; (2) determine the number of output layer neurons; (3) initialization of weights and initial bias; (4) performance of network training on training data; (5) performance of network testing using test data; and (6) model validation.

### 2.5.4 Surface runoff

Accurate surface runoff estimation is one of the most fundamental and important points for planning and managing water resources and assessing the environmental quality of soil and water [43]. Several methods are available to determine surface runoff, namely the rational, Green-Ampt, and SCS-CN methods [44]. In this study, surface runoff was calculated using the SCS-CN method equation (Eq. (11)) because it is easy to apply and considers all catchment factors that influence runoff [45], and is suitable for small watersheds with an area of  $\leq 250 \text{ km}^2$  [46]. This method is a popular rainfall-runoff model used to estimate losses and runoff directly from rainfall events [47].

$$R = \frac{(P - 0.2S)^2}{P + 0.8S} \quad (11)$$

where,  $P$  is rainfall;  $S$  is a retention parameter that describes the maximum potential for rainfall to be infiltrated or become runoff. The  $S$  value is calculated by Eq. (12).

$$S = 25.4 \times \left( \frac{1000}{CN} - 10 \right) \quad (12)$$

### 3. RESULTS AND DISCUSSION

#### 3.1 Land cover changes

The results of the GIS analysis show several types of land cover in the Citarum-Majalaya catchment. Based on SNI 7645 2010, they are classified into forest land, agriculture, plantations, settlements, bushes, water bodies, and open land. Figure 9 shows a comparison of land cover conditions in 2000 and 2021. During this period, land cover, especially

settlements, appears to have changed very significantly and relatively quickly compared to changes in other types of land cover. More detailed data can be seen in Table 5. The area of forest land shows a decreasing trend of change (decreased of 3.7%); Agricultural land also shows a decreasing trend of change (decreased of 5.7%); and residential land area data (built-up areas) shows an increasing trend and a very significant increase (an increase of 129%). The forest area in the location is lower than 30%. In comparison, the forest area must be maintained at least 30% (thirty percent) of the watershed or catchment area [48]. The area of forest land, which decreases linearly, and residential land, which continues to increase exponentially in the long term, will have an impact on water availability in the Bandung Basin.

**Table 5.** Land cover of the Citarum-Majalaya catchment 2000-2021

Years	Area/Percentage	Land Cover					
		Forest	Agriculture	Settlements	Shrubs	Open Land	Water Bodies
2000	km <sup>2</sup>	59.6	130.4	8.6	2.3	3.5	0.1
	%	29.1	63.8	4.2	1.1	1.7	0.1
2003	km <sup>2</sup>	59.6	130.9	9.5	2.6	1.7	0.1
	%	29.1	64.0	4.6	1.3	0.9	0.1
2006	km <sup>2</sup>	59.4	129.6	10.8	2.9	1.7	0.1
	%	29.0	63.4	5.3	1.4	0.9	0.1
2009	km <sup>2</sup>	58.5	128.6	12.6	2.9	1.8	0.1
	%	28.6	62.9	6.2	1.4	0.9	0.1
2012	km <sup>2</sup>	58.4	128.5	13.5	1.9	2.1	0.2
	%	28.6	62.8	6.6	0.9	1.0	0.1
2015	km <sup>2</sup>	58.4	127.7	15.8	0.6	1.8	0.2
	%	28.5	62.5	7.7	0.3	0.9	0.1
2018	km <sup>2</sup>	57.6	126.0	18.7	0.9	1.2	0.2
	%	28.2	61.6	9.1	0.4	0.6	0.1
2021	km <sup>2</sup>	57.4	122.9	19.8	3.8	0.3	0.2
	%	28.1	60.1	9.7	1.9	0.2	0.1

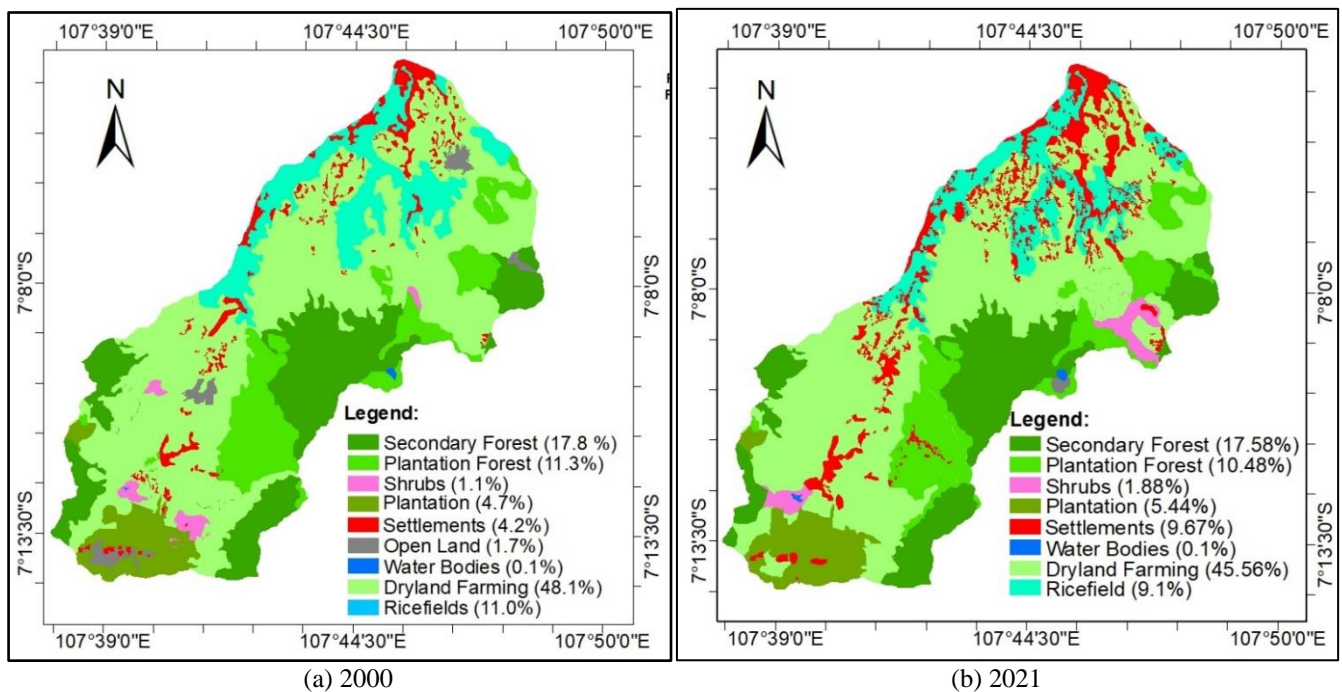


**Figure 9.** Land cover of the Citarum-Majalaya catchment

Figure 10 shows the trend in land cover changes over a period of 22 years from 2000-2021. The analysis uses corrected land cover map data from the Ministry of Environment and Forestry. Figure 10(a) shows the trend of

forest land change, which decreases linearly, even though the rate of change is relatively small. The exponential trend in Figure 10(b) shows a very rapid increase in residential land cover over time, and Figure 10(c) shows a decreasing trend in



changes in agricultural land cover following the quadratic equation. Other land cover, such as shrubs and open land, appears to be fluctuating and does not show a particular pattern. Changes in land cover are dynamic, along with changes as a result of increasing demands for land.

The analysis of land cover changes in this study yielded results that differ considerably from those reported in previous research [2]. These discrepancies are likely attributable to the use of land cover maps in earlier studies that may not have undergone thorough spatial correction and classification processes. Notable differences are particularly evident in the patterns and extent of land cover change, especially within the categories of built-up areas (settlements), forest, and agricultural land.

Previous studies have indicated that land cover changes over specific time periods tended to be minor and lacked a consistent pattern. For instance, residential land cover

remained relatively stable over a 12-year period (2000–2012), followed by a slight decline between 2012 and 2014. However, the reliability of these dynamics is questionable, given that field observations indicate a rapid increase in population accompanied by the expansion of socio-economic activity.

Similarly, forest cover during the 2000–2009 period and agricultural land between 2000 and 2006 appeared relatively constant, which does not correspond with observed field dynamics. In contrast, the analysis based on land cover maps that have undergone correction processes reveals a more logical and systematic pattern of change, as illustrated in Figure 10. Over a 21-year period (2001–2021), forest cover exhibits a linear trend, while residential and agricultural land display exponential and quadratic polynomial trends, respectively. A comparison of the impact of land cover changes on Curve Number (CN) values is presented in Figure 11.

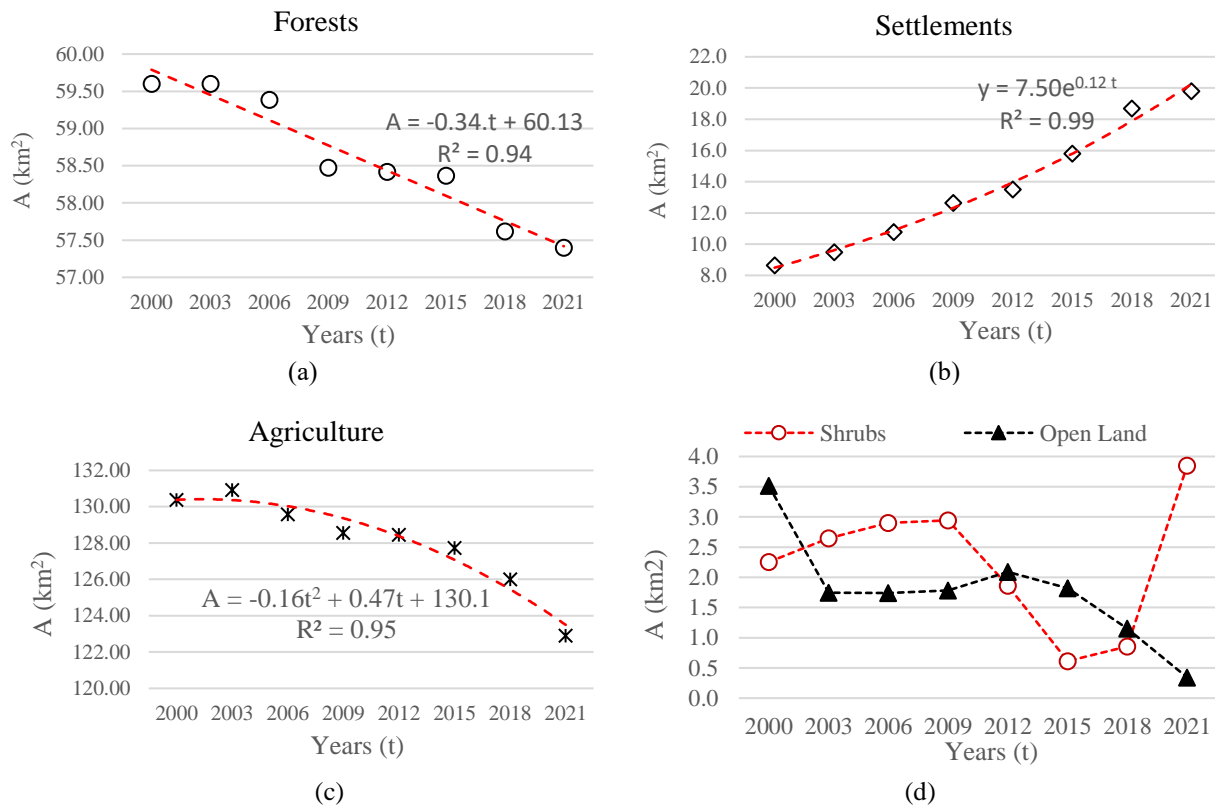


Figure 10. Land cover trends (2000-2021) (a) Forests; (b) Settlements; (c) Agriculture; (d) Shrubs and open land

Table 6. Variation in land cover changes between 2000-2021

Study Phase	Single Land Cover Type Dynamic Index K					Comprehensive Land Cover Type Dynamic Index Lc	
	Forest	Agriculture	Settlements	Shrubs	Open Land	Water Bodies	
2000-2006	-0.06	-0.10	4.26	4.35	-8.57	0.00	0.23
2006-2012	-0.28	-0.14	4.17	-5.75	3.92	16.67	0.26
2012-2018	-0.23	-0.32	6.42	-8.77	-7.14	0.00	0.42
2018-2021	-0.12	-0.82	1.96	107.41	-25.00	0.00	0.67

During 2000-2021, various types of land cover experienced changes in varying degrees. The results of data processing on variations in land cover changes in the 2000, 2006, 2012, 2018, and 2021 phases are presented in Table 6.

The rate of comprehensive land cover dynamics for each phase tends to increase. Sequentially, it is 0.23% from 2000 to 2006, 0.26% from 2006 to 2012, 0.42% from 2012 to 2018, and 0.67% from 2018 to 2021. Based on the rate of single land cover dynamics, the largest variation sequentially occurs in

open land, which is -8.57% (2000-2006), water bodies are 16.67% (2006-2012), shrubs are -8.77% (2012-2018), and shrubs is 107.41 (2018-2021). Based on the overall rate of single land cover dynamics for each phase, it is known that forest and agricultural land in each phase have variations that tend to decrease, while settlements have variations that tend to increase. Shrubs and open land have higher levels of variation than other types of land cover and tend to be uncertain.

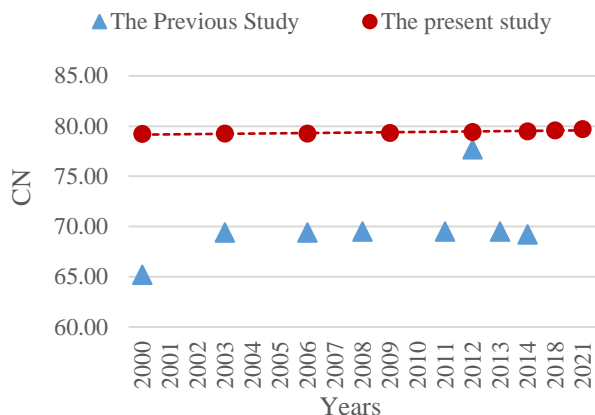


Figure 11. CN comparison

### 3.2 CN changes

The CN value over 22 years (2000-2021) in a three-year time interval, and the changing trend can be seen in Figure 12. The CN value over time appears to change at varying rates and follows certain patterns. Visually, it appears that the changes have a linear trend, but if identified more carefully, it will be closer to a quadratic trend pattern and has an  $R^2$  value that is closer to 1, namely 0.994, while the linear trend has an  $R^2$  value is 0.989. The quadratic trend model for the CN value of the Citarum-Majalaya catchment is expressed in the form of Eq. (13).

$$CN = 0.009t^2 - 0.009t + 79.223 \quad (13)$$

where,  $t$  is time (year) and  $CN$  is the predicted  $CN$  value on the trend line.

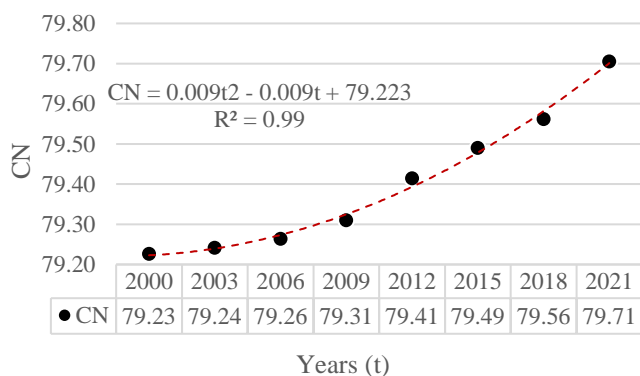


Figure 12. CN value trend of the Citarum-Majalaya catchment (2000-2021)

The increase in the CN value in the period 2000-2006 appears relatively less significant, namely only ranging between 79.23-79.26. However, in the following time period between 2009-2021, the increase in the CN value was more significant, ranging from 79.26 to 79.7. The pattern of changes in CN values is relevant to patterns of land cover change, in particular changes in the area of forest land cover, settlements (built environment), and agriculture. The decrease in the area of forest land and agricultural land and the increase in the area of residential land (built environment) have an effect on increasing the CN value. Regarding the trend in CN values,

previous research concluded that in the period 1999-2016, the CN values in the Citarum-Majalaya catchment tended not to change. The increase in maximum discharge in this study was more influenced by the increase in rainfall. This is suspected to have an influence due to the use of uncorrected land cover maps.

The differences in land cover change dynamics, as compared to previous studies, also influence the variability of the Curve Number (CN) values. In the present study, CN values derived from land cover maps that underwent a correction process exhibit a more stable pattern of change, following both linear and quadratic trends. In contrast, CN values reported in earlier studies tend to be lower and display inconsistent fluctuations. These patterns are illustrated in Figure 11.

### 3.3 Projection of CN value

The projection of the CN value of the Citarum-Majalaya catchment was made over 29 years (2022-2050). It's calculated using Eq. (9) through two approaches. The first assumes that there is no action was taken related to land cover control and planning during that period. The second is a land cover scenario based on the 2024-2044 spatial pattern plan [49].

The land cover scenario was created based on Law no. 42/1989 concerning forestry, which explains that the minimum forest area that must be maintained is 30% of the watershed area [48]. It's also based on the spatial pattern plan by the Bandung Regency Spatial Plan for 2024-2044 [49]. Projections assume that land cover in 2044 will be based on the spatial pattern plan and will become a reference for land cover scenarios in other years. Based on spatial pattern plan map data (Figure 6), it is known that there are several plans for designated areas in the catchment in 2044. For analysis purposes, they are grouped into six (6) groups of land cover plans (Table 7). Area plans for horticulture, food crops, and livestock are grouped into agricultural area plans; Protected forest areas, nature reserves, and natural tourism parks are grouped into forest areas; and planned areas for rural settlements, urban settlements, tourism, and industry are grouped into built-up areas (settlements).

Table 7. Classification of land cover types is based on the 2044 spatial pattern plan

Area Plan	Land Area	
	km <sup>2</sup>	%
Settlements (Built environment)	27.988	13.685
Forest	98.159	47.995
Plantation	38.882	19.011
Agriculture	38.334	18.743
Water bodies	0.280	0.137
Local protection	0.684	0.335
Other	0.192	0.094
<b>Total</b>	<b>204.52</b>	<b>100.00</b>

Land cover scenarios are created using trend models for each type of land cover. They are based on combined data from actual land cover in 2000-2021 and spatial pattern plan data in 2044. The scenario trend model for each land cover is presented in Figure 10. Based on the trend, a land cover scenario was created for 27 years (2024-2050). Scenario data for forest land area and other land uses for projected CN values are presented in Table 8.

**Table 8.** Scenario of land cover for 2024-2050

Years	Forest (km <sup>2</sup> )	Settlements (km <sup>2</sup> )	Plantation (km <sup>2</sup> )	Agriculture (km <sup>2</sup> )	Water Bodies (km <sup>2</sup> )
2024	62.67	20.43	15.56	105.62	0.24
2027	65.78	21.73	17.73	99.03	0.24
2030	69.55	22.96	20.28	91.48	0.25
2033	73.99	24.13	23.19	82.95	0.26
2036	79.09	25.23	26.47	73.46	0.27
2039	84.86	26.27	30.11	63.00	0.28
2042	91.29	27.24	34.13	51.59	0.28
2044	98.84	27.99	38.88	38.53	0.28
2047	98.84	29.00	38.88	37.52	0.28
2050	98.84	29.78	38.88	36.74	0.28

The projected CN value based on scenarios (CNs) for 2024-2050 is smaller than the CN value with no effort (CNd). The CNs value in 2044, assuming that the allotment area plan is realized according to the spatial pattern plan, is estimated to have a value of 79.87, while the CNs value is 81.51. Regarding the pattern of changes in CN values, it appears that CNs have a smaller trend of increasing value compared to the rate of increase in CNd values, where the CNs value in 2050 is 79.93 (still < 80) while the CNd value is higher (82.17). A comparison graph of the CN values resulting from the two approaches can be seen in Figure 13.

Response to the trend of changes in the CN value of the scenario, which is still relatively increasing, even though the forest area is higher than 30% of the catchment area. It is allegedly due to the residential area (built-up area), which also continues to increase according to the spatial pattern plan.

The results of the t-test at a significance level of  $\alpha = 0.05$  yielded a calculated t-value of -0.853, which is greater than the critical t-value of -2.15. Therefore, it can be concluded with 95% confidence that the projected CN value is not significantly different from the observed CN value. This indicates that the CN model derived from the first approach is valid and can be used for future CN value projections. Similarly, the model performance evaluation resulted in a Mean Absolute Percentage Error (MAPE) of 0.18%, which is well below the 10% threshold, indicating excellent model

performance in predicting CN values. Furthermore, in the comparison between the two different approaches, the t-test produced a calculated t-value of 4.98, exceeding the critical value of 2.15. This result suggests a statistically significant difference in the CN values generated by the two approaches.

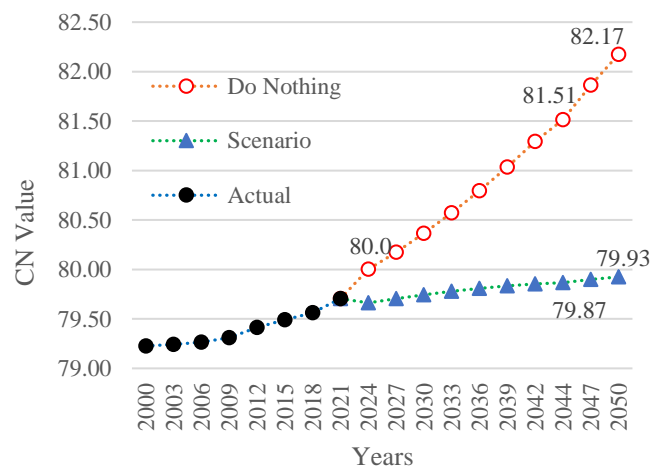


**Figure 13.** Projected CN value for the Citarum-Majalaya catchment in 2021-2050

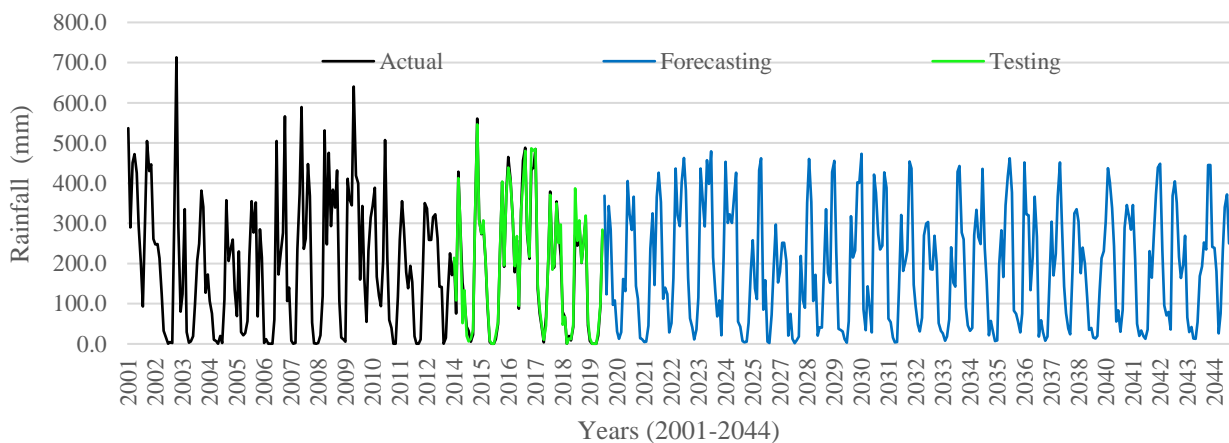


**Figure 14.** Graph of monthly rain forecasting data in 2020-2044

### 3.4 Forecasting monthly rainfall

Monthly rainfall is forecasted using the ANN-BP with historical data over 22 years (2001-2021). The data is divided

into two parts: training and testing data. There are several proportions of training data and testing data [50], and in this study, the data was divided into 60% for the training process and 40% for the testing process. The forecasting is calculated

using the Simulink-Matlab R2021a application. The best network architecture for forecasting: one (1) input layer, one (1) hidden layer with six (6) neurons, and one (1) output layer. Plots of monthly forecasting data are presented in Figure 14. Based on the value of the goodness of the model using several statistical measurement criteria (MAPE=19.8%, RMSE=0.15 and NSE=0.97) and the results of the model performance test (MAPE=45.1%, RMSE=0.29 and NSE=0.31), it was concluded that the forecasting results were quite good so it can be used to calculate surface runoff discharge.

### 3.5 Surface runoff

The impact of actual land cover change on the Curve Number (CN) and surface runoff volume was analyzed using an assumed rainfall depth of 100 mm. Land cover changes over a 22-year period, from 2000 to 2021 (Table 5), resulted in an increase in the CN value by 0.5, from 79.2 in 2000 to 79.7 in 2021. Based on the same rainfall assumption, the surface runoff depth increased from 49 mm in 2000 to 50 mm in 2021. When converted into runoff volume using a catchment area of 204.52 km<sup>2</sup>, the volume rose from 10,027,141 m<sup>3</sup> in 2000 to 10,217,258 m<sup>3</sup> in 2021, indicating an increase of 190,117 m<sup>3</sup> during this period. Furthermore, based on the projected CN value, which is estimated to reach 81.51 by 2044, and assuming the same rainfall depth of 100 mm, the surface runoff depth is projected to reach 51.9 mm. This corresponds to a runoff volume of 10,611,927 m<sup>3</sup>. Accordingly, there is a projected increase of 394,669 m<sup>3</sup> in runoff volume during the period from 2021 to 2044, with a cumulative increase of 584,786 m<sup>3</sup> when compared to the conditions in the year 2000.

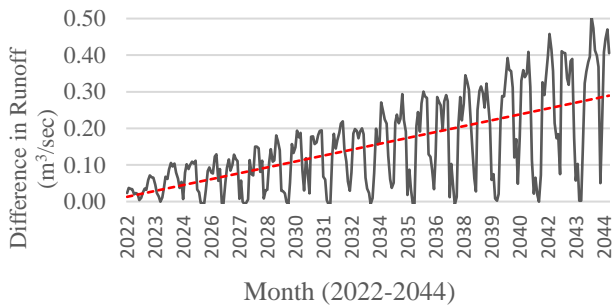
A comparative analysis of the impact of land cover change projections based on two different approaches was conducted to evaluate surface runoff, using monthly rainfall data obtained through forecasting. The projected monthly rainfall data, along with the projected Curve Number (CN) values, were used as inputs for the SCS-CN method to estimate surface runoff over a 24-year period, from 2021 to 2044. The analysis revealed that surface runoff calculated using CN values from the first approach (CNd) was consistently higher than that derived from the second approach (CNs). The difference in runoff between the two approaches showed a growing trend in line with the increasing disparity in CN values over time (Figure 15). The maximum runoff generated using CNs in 2025 was recorded at 28.18 m<sup>3</sup>/s, while the value based on CNd reached 28.29 m<sup>3</sup>/s, indicating a difference of 0.11 m<sup>3</sup>/s for that year. This difference continued to increase and reached 0.51 m<sup>3</sup>/s by the year 2044.

The CNd (do-nothing) value shows that if there are no efforts related to land cover control and planning, we will face decreasing hydrological conditions in the future. Surface runoff will increase rapidly from time to time, along with changes in catchment characteristics, especially related to land cover. The impact of increased surface runoff in a hydrological context will be felt directly and indirectly by the community. The impact such as increasing peak discharge and flood frequency, the risk of soil erosion, damage to infrastructure, a decrease in groundwater availability due to reduced infiltration capacity, degradation of water quality, and other adverse impacts.

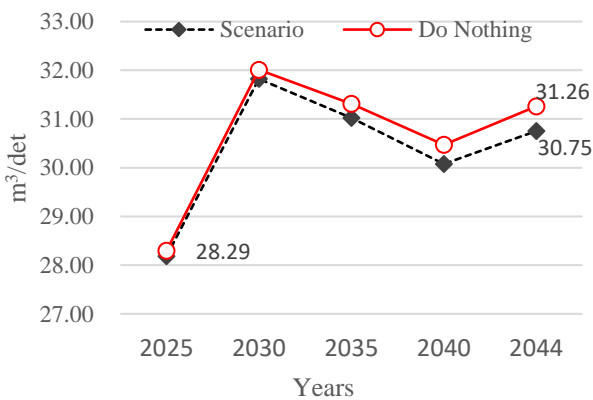
The trend changes in CN values are still relatively increasing, even though the forest area in the scenario exceeds 30%. This illustrates that an integrated and comprehensive approach is needed in efforts to control CN values. They are between vegetation scenarios and other sustainable regional development scenarios to obtain effective results.

Another approach that can be applied to control the CN value is to apply conservation methods to land that has a slope of more than 25%. Applying appropriate conservation methods with attention to slope can reduce surface runoff, increase infiltration, and prevent soil erosion [9]. This needs to be done considering that agricultural land in the catchment area in 2021, which has a slope > 25%, is quite extensive. There are around 28.43 km<sup>2</sup> or 13.9% of the total area of the catchment. Whereas in 2044, assuming the spatial pattern plan is maximally realized will be reduced to around 10.97 km<sup>2</sup> or 5.4% of the total water catchment area. The decrease in agricultural land area occurred due to the conversion to forest land, especially agricultural land with a slope of > 25%. Conservation techniques such as swales, bund terraces, and bench terraces can be applied to land with a slope of > 25% to reduce surface runoff and prevent soil erosion [51].

The discussion of the relationship between corrected land cover changes and their impact on surface runoff, as projected through variations in the CN, can offer significant contributions to watershed management and the development of water resource management policies. This study presents three key contributions that are particularly relevant: 1) The utilization of spatially corrected land cover maps yields more accurate and representative projections of CN values, better reflecting actual field conditions. This improvement enhances the reliability of surface runoff estimations, which is essential for the effective planning and design of water resource infrastructure; 2) This study contributes to a deeper understanding of how land cover changes influence the



(a) The trend of differences in surface runoff



(b) Maximum surface runoff

**Figure 15.** The trend of differences in surface runoff from the two CN value approaches

hydrological behavior of watersheds. Such insight is essential for predicting flood risks based on observed trends in land cover change; 3) The findings of this study may serve as a valuable reference for reviewing the Regional Spatial Planning Plan. More accurate and context-specific CN value information can support decision-making in regulating development permits, particularly in areas with high surface runoff potential.

#### 4. CONCLUSIONS

Land cover dynamics exert a significant influence on the Curve Number (CN) value. Projections for the CN value over the period 2024–2044 indicate that land cover control and spatial planning, particularly through the implementation of spatial pattern plans that ensure a minimum of 30% forest cover within a river basin (DAS), lead to a reduction in the CN value. According to these projections, the CN value is expected to reach 79.87 by 2044 and 79.93 by 2050, remaining below the critical threshold of 80.00, assuming that the spatial pattern plan is effectively implemented in line with the designated land use allocations. In contrast, the second scenario, which does not prioritize such strict spatial planning, estimates a CN value of 81.52 in 2044, which increases to 82.17 by 2050. These findings highlight the importance of integrated land cover planning and control, underpinned by appropriate spatial policies, in significantly reducing the CN value and mitigating associated hydrological risks.

An increase in the Curve Number (CN) value has a direct effect on the rise in surface runoff. Comparative analysis between two different land management scenarios reveals a consistent upward trend in surface runoff over time. In 2025, the maximum runoff under the controlled CN scenario was recorded at 28.18 m<sup>3</sup>/second, whereas the scenario without intervention reached 28.29 m<sup>3</sup>/second, resulting in a difference of 0.11 m<sup>3</sup>/second. This disparity widens progressively, reaching 0.51 m<sup>3</sup>/second by 2044, and is projected to further increase by 2050. These results suggest that in the absence of land cover control and appropriate spatial planning, future hydrological conditions are likely to deteriorate. The projected increase in surface runoff poses potential risks, both direct and indirect, which may have significant implications for communities within the affected areas.

Although the second scenario includes a forest cover exceeding 30% of the total watershed (DAS) area and incorporates various land cover control and planning measures, the projected Curve Number (CN) values under this scenario continue to exhibit an increasing trend. This indicates that the current efforts may not be sufficient to effectively regulate CN values over time. Consequently, the adoption of additional and more effective strategies is necessary to enhance CN control. One recommended measure is the implementation of land conservation practices, particularly on areas with slopes greater than 25%. Such interventions can significantly reduce surface runoff potential and improve the soil's water infiltration capacity.

This study yields several key insights with practical applications, particularly in the context of spatial and environmental planning. First, information on changes in the Curve Number (CN) resulting from land cover dynamics can assist spatial planners in identifying areas that are increasingly susceptible to surface runoff and flood hazards. Such information serves as a valuable basis for formulating land

zoning policies that are more adaptive to hydrological risks. Second, data reflecting increased runoff responses due to land cover changes can inform the planning and design of drainage systems and spatial layouts, with the objective of minimizing surface runoff volumes and improving flood resilience. Third, the projected CN and surface runoff values can be utilized as inputs in the development of future flood prediction models, particularly those that incorporate various land cover change scenarios. This data and associated findings can support local governments in formulating regional regulations concerning the protection and management of river basins (DAS) or catchment areas, especially within the study regions.

Further research is recommended to examine the combined effects of land cover scenarios based on the Regional Spatial Planning Plan and the implementation of conservation practices on areas with slopes exceeding 25%. This approach aims to provide a more comprehensive understanding of the strategies for controlling Curve Number (CN) values and surface runoff within the Citarum–Majalaya Catchment.

#### ACKNOWLEDGMENT

The authors would like to express their sincere gratitude to the Dean of the Faculty of Civil and Environmental Engineering (FTSL), Institut Teknologi Bandung (ITB), as well as the Water Resources Engineering Research Group and the Postgraduate Program in Civil Engineering at ITB, for their valuable support and permission to conduct this research.

Special thanks are also extended to the Ministry of Environment and Forestry of Indonesia for providing essential land cover data for the Citarum watershed.

#### REFERENCES

- [1] Burnama, N.S., Rohmat, F.I.W., Farid, M., Kuntoro, A.A., Kardhana, H., Rohmat, F.I.W., Wijayasari, W. (2023). The utilization of satellite data and machine learning for predicting the inundation height in the Majalaya watershed. *Water*, 15(17): 3026. <https://doi.org/10.3390/w15173026>
- [2] Rizaldi, A., Kusuma, M.S.B., Kuntoro, A.A., Kardhana, H. (2022). Trend analysis of rainfall, land cover, and flow discharge in the Citarum Hulu–Majalaya Basin. *International Journal on Advanced Science, Engineering and Information Technology*, 12(4): 1469-1477.
- [3] Lin, K., Lv, F., Chen, L., Singh, V.P., Zhang, Q., Chen, X. (2014). Xinanjiang model combined with Curve Number to simulate the effect of land use change on environmental flow. *Journal of Hydrology*, 519: 3142-3152. <https://doi.org/10.1016/j.jhydrol.2014.10.049>
- [4] Cihlar, J., Jansen, L.J. (2001). From land cover to land use: A methodology for efficient land use mapping over large areas. *The Professional Geographer*, 53(2): 275-289. <https://doi.org/10.1080/00330124.2001.9628460>
- [5] Lillesand, T., Kiefer, R.W., Chipman, J. (2015). *Remote Sensing and Image Interpretation*. John Wiley & Sons. <https://doi.org/10.2307/634969>
- [6] Onyango, D.O., Ikporukpo, C.O., Taiwo, J.O., Opiyo, S.B. (2021). Land use and land cover change as an indicator of watershed urban development in the Kenyan Lake Victoria Basin. *International Journal of Sustainable Development and Planning*, 16(2): 335-345.

- <https://doi.org/10.18280/IJSDP.160213>
- [7] Kuntoro, A.A., Putro, A.W., Kusuma, M.S.B., Natasaputra, S. (2017). The effect of land use change to maximum and minimum discharge in Cikapundung River Basin. *AIP Conference Proceedings*, 1903(1): 100011. <https://doi.org/10.1063/1.5011621>
- [8] Farid, M., Pratama, M.I., Kuntoro, A.A., Adityawan, M.B., Rohmat, F.I.W., Moe, I.R. (2022). Flood prediction due to land cover change in the Ciliwung River Basin. *International Journal of Technology*, 13(2): 356-366. <https://doi.org/10.14716/ijtech.v13i2.4662>
- [9] Kuntoro, A.A., Cahyono, M., Soentoro, E.A. (2018). Land cover and climate change impact on river discharge: Case Study of upper Citarum river basin. *Journal of Engineering & Technological Sciences*, 50(3): 364-381. <https://doi.org/10.5614/j.eng.technol.sci.2018.50.3.4>
- [10] Kumar, A., Kanga, S., Taloor, A.K., Singh, S.K., Durin, B. (2021). Surface runoff estimation of Sind river basin using integrated SCS-CN and GIS techniques. *HydroResearch*, 4: 61-74. <https://doi.org/10.1016/j.hydres.2021.08.001>
- [11] Mucbe, M.E., Hutchinson, S.L., Hutchinson, J.S., Johnston, J.M. (2019). Phenology-adjusted dynamic curve number for improved hydrologic modeling. *Journal of Environmental Management*, 235: 403-413. <https://doi.org/10.1016/j.jenvman.2018.12.115>
- [12] Ajmal, M., Waseem, M., Jehanzaib, M., Kim, T.W. (2023). Development and testing of updated curve number models for efficient runoff estimation in steep-slope watersheds. *Journal of Hydrology*, 617: 129049. <https://doi.org/10.1016/j.jhydrol.2022.129049>
- [13] Shi, W., Wang, N. (2020). An improved SCS-CN method incorporating slope, soil moisture, and storm duration factors for runoff prediction. *Water*, 12(5): 1335. <https://doi.org/10.3390/w12051335>
- [14] Wardhana, P.N., Yuni, S.A., Kurnia, D. (2018). Pengaruh perubahan tutupan lahan terhadap debit banjir di DAS winongo daerah istimewa Yogyakarta. *Jurnal Ilmiah Teknik Sipil*, 22(2): 157-164.
- [15] Ayumi, N., Cristianto, N. (2022). Analysis of the effect of land cover change on surface runoff using HEC-HMS in the Gajahwong Watershed, Yogyakarta in 2016 and 2020. *Gajah Mada University*. <http://etd.repository.ugm.ac.id/>.
- [16] Pribadi, A.D., Kusumawati, R.D., Firdausi, A.A. (2021). Pengaruh perubahan tutupan lahan terhadap karakteristik hidrologi di DAS Sampean Kabupaten Bondowoso. *Jurnal Ilmiah Desain & Konstruksi*, 19(2): 84-101. <https://doi.org/10.35760/dk.2020.v19i2.3492>
- [17] Zainah, N., Maulana, M.A., Margini, N.F. (2024). Pengaruh perubahan tata guna lahan terhadap nilai curve number Pada DAS Sarokah. *Jurnal Ilmiah MITSU*, 12(2). <https://doi.org/10.24929/ft.v12i2.3612>
- [18] Wisanggeni, D.H., Sitorus, J.E., Putra, K.H.P., Adityawan, M.B. (2024). Pengaruh perubahan tutupan lahan terhadap debit banjir di kawasan Inti Pusat Pemerintahan (KIPP) Ibu Kota Nusantara. *Jurnal Teknik Sipil dan Lingkungan*, 9(2): 327-338.
- [19] Farid, M., Pratama, M.I., Kuntoro, A.A., Adityawan, M.B., Rohmat, F.I.W., Moe, I.R. (2021). Pengaruh perubahan tutupan lahan terhadap debit banjir di daerah aliran Sungai Ciliwung Hulu. *Jurnal Teknik Sipil*, 28(3): 309-318.
- [20] Romlah, D.R., Yuwono, S.B., Hilmanto, R., Banuwa, I.S. (2018). Pengaruh perubahan tutupan hutan terhadap debit Way Seputih Hulu. *Jurnal Hutan Tropis*, 6(2): 197-204. <https://doi.org/10.20527/jht.v6i2.5408>
- [21] Achmad, A., Ramli, I., Sugiarto, S., Irzaidi, I., Izzaty, A. (2024). Assessing and forecasting carbon stock variations in response to land use and land cover changes in Central Aceh, Indonesia. *International Journal of Design & Nature and Ecodynamics*, 19(2): 465-475. <https://doi.org/10.18280/ijdne.190212>
- [22] Taye, G., Vanmaercke, M., van Wesemael, B., Tesfaye, S., Teka, D., Nyssen, J., Deckers, J., Poesen, J. (2023). Estimating the runoff response from hillslopes treated with soil and water conservation structures in the semi-arid Ethiopian highlands: Is the curve number method applicable? *Scientific African*, 20: e01620. <https://doi.org/10.1016/j.sciaf.2023.e01620>
- [23] Standar Nasional Indonesia. (2010). SNI 7645:2010 Standar Nasional Indonesia Klasifikasi penutup lahan.
- [24] Bhattacharya, R.K., Chatterjee, N.D., Das, K. (2020). An integrated GIS approach to analyze the impact of land use change and land cover alteration on ground water potential level: A study in Kangsabati Basin, India. *Groundwater for Sustainable Development*, 11: 100399. <https://doi.org/10.1016/j.gsd.2020.100399>
- [25] Nithya, C.N., Srinivas, Y., Magesh, N.S., Kaliraj, S. (2019). Assessment of groundwater potential zones in Chittar basin, Southern India using GIS based AHP technique. *Remote Sensing Applications: Society and Environment*, 15: 100248. <https://doi.org/10.1016/j.rsase.2019.100248>
- [26] Wang, H.Q., Cheng, S. (2020). Spatiotemporal variation in land use of Northeast China Tiger and Leopard National Park. *International Journal of Design & Nature and Ecodynamics*, 15(6): 835-842. <https://doi.org/10.18280/ijdne.150609>
- [27] Ross, C.W., Prihodko, L., Anchang, J., Kumar, S., Ji, W., Hanan, N.P. (2018). Global hydrologic soil groups (HYSOgs250m) for curve number-based runoff modeling. ORNL DAAC, Oak Ridge, Tennessee, USA. <https://doi.org/10.3334/ORNLDAAC/1566>
- [28] Hong, Y., Adler, R.F., Hossain, F., Curtis, S., Huffman, G.J. (2007). A first approach to global runoff simulation using satellite rainfall estimation. *Water Resources Research*, 43(8). <https://doi.org/10.1029/2006WR005739>
- [29] Gebresellassie Zelelew, D. (2017). Spatial mapping and testing the applicability of the curve number method for ungauged catchments in Northern Ethiopia. *International Soil and Water Conservation Research*, 5(4): 293-301. <https://doi.org/10.1016/j.iswcr.2017.06.003>
- [30] USDA. (1986). *Urban Hydrology for Small Watersheds*. Soil Conservation Service, USDA, Washington DC.
- [31] Ideawati, L.F., Limantara, L.M., Andawayanti, U. (2015). Analisis perubahan bilangan kurva aliran permukaan (runoff curve number) terhadap debit banjir di das lesti. *Jurnal Teknik Pengairan*, 6(1): 37-45.
- [32] Tikno, S., Hariyanto, T., Anwar, N., Karsidi, A., Aldrian, E. (2012). Aplikasi metode Curve Number untuk mempresentasikan hubungan curah hujan dan aliran permukaan di DAS Ciliwung Hulu-Jawa Barat. *Jurnal Teknologi Lingkungan*, 13(1): 25-36.
- [33] Triatmodjo, B. (2019). *Hidrologi Terapan*. Beta Offset, Yogyakarta.
- [34] Yonhy, Y., Goejantoro, R., Wahyuningsih, S. (2013).

- Metode trend non linear untuk forecasting jumlah keberangkatan tenaga kerja Indonesia di Kantor imigrasi kelas II kabupaten nunukan. *Jurnal Eksponensial*, 4(1): 47-54.
- [35] Mohseni, F., Jamali, S., Ghorbanian, A., Mokhtarzade, M. (2023). Global soil moisture trend analysis using microwave remote sensing data and an automated polynomial-based algorithm. *Global and Planetary Change*, 231: 104310. <https://doi.org/10.1016/j.gloplacha.2023.104310>
- [36] Naabil, E., Lamptey, B.L., Arnault, J., Olufayo, A., Kunstmann, H. (2017). Water resources management using the WRF-Hydro modelling system: Case-study of the Tono dam in West Africa. *Journal of Hydrology: Regional Studies*, 12: 196-209. <https://doi.org/10.1016/j.ejrh.2017.05.010>
- [37] Lian, H., Yen, H., Huang, J.C., Feng, Q., Qin, L., et al. (2020). CN-China: Revised runoff curve number by using rainfall-runoff events data in China. *Water Research*, 177: 115767. <https://doi.org/10.1016/j.watres.2020.115767>
- [38] Yudha, S., Dibyosaputro, S. (2013). Dampak perubahan penggunaan lahan terhadap perubahan runoff di daerah aliran sungai (DAS) bedog yogyakarta. *MGI*, 28: 117-137.
- [39] Fausett, L.V. (2006). *Fundamentals of Neural Networks: Architectures, Algorithms and Applications*. Pearson Education India.
- [40] Nugraha, H.G., Azhari, S.N. (2014). Optimasi bobot jaringan syaraf tiruan menggunakan particle swarm optimization. *Indonesian Journal of Computing and Cybernetics Systems*, 8(1): 25-36. <https://doi.org/10.22146/ijccs.3492>
- [41] Rumelhart, D.E., Hinton, G.E., Williams, R.J. (1986). learning representations by back-propagatings errors. *Nature*, 323(6088): 533-536. <https://doi.org/10.1038/323533a0>
- [42] Windarto, A.P., Lubis, M.R., Solikhun, S. (2018). Model arsitektur backpropagation pada prediksi total laba rugi komprehensif bank umum konvensional dalam mendorong laju pertumbuhan ekonomi. In *Prosiding Seminar Rekayasa Teknologi (SemResTek)*, pp. 330-338.
- [43] Lal, M., Mishra, S.K., Kumar, M. (2019). Reverification of antecedent moisture condition dependent runoff curve number formulae using experimental data of Indian watersheds. *Catena*, 173: 48-58. <https://doi.org/10.1016/j.catena.2018.09.002>
- [44] Jaafar, H.H., Ahmad, F.A., El Beyrouthy, N. (2019). GCN250, new global gridded curve numbers for hydrologic modeling and design. *Scientific Data*, 6(1): 145. <https://doi.org/10.1038/s41597-019-0155-x>
- [45] Uwizeyimana, D., Mureithi, S.M., Mvuyekure, S.M., Karuku, G., Kironchi, G. (2019). Modelling surface runoff using the soil conservation service-curve number method in a drought prone agro-ecological zone in Rwanda. *International Soil and Water Conservation Research*, 7(1): 9-17. <https://doi.org/10.1016/j.iswcr.2018.12.001>
- [46] Sentosa, A.K., Asdak, C., Suryadi, E. (2021). Estimasi volume limpasan dan debit puncak sub DAS cikeruh menggunakan metode SCS-CN (Soil conservation service-curve number). *Journal of Tropical Agricultural Engineering and Biosystems-Jurnal Keteknikaan Pertanian Tropis dan Biosistem*, 9(1): 90-98. <https://doi.org/10.21776/ub.jkptb.2021.009.01.10>
- [47] Petroselli, A., Grimaldi, S., Romano, N. (2013). Curve-Number/Green-Ampt mixed procedure for net rainfall estimation: A case study of the Mignone watershed, IT. *Procedia Environmental Sciences*, 19: 113-121.
- [48] Pemerintah Republik Indonesia. (1999). Undang-Undang Republik Indonesia No. 41 Tahun 1999 tentang Kehutanan. Presiden Republik Indonesia.
- [49] Pemerintah Daerah Kabupaten Bandung. (2024). Bandung regency regional regulation number 1 of 2024 concerning the Bandung regency regional spatial plan for 2024-2044. Local Government of Bandung Regency. <https://wargi.jabarprov.go.id/download/read/peraturan-daerah-kabupaten-bandung-nomor-1-tahun-2024-tentang-rencana-tata-ruang-wilayah-kabupaten-bandung-tahun-20242044>.
- [50] Rozenberg, G., Bäck, T., Kok, J.N. (2012). *Handbook of Natural Computing*. Springer Berlin Heidelberg. <https://doi.org/10.1007/978-3-540-92910-9>
- [51] Pemerintah Republik Indonesia. (2014). Law (UU) number 37 of 2014 concerning soil and water conservation. Indonesia, Central Government. <https://peraturan.bpk.go.id/Details/38775/uu-no-37-tahun-2014>.